RSC Advances

PAPER

View Article Online
View Journal | View Issue

Check for updates

Cite this: *RSC Adv.*, 2025, **15**, 39975

Green-synthesized silver nanoparticles for improved heat stress resilience and germination in potato seeds

Jakia Mustary Lina,†[a] Md. Shadman Mostafa, †[bcd] Samia Yeasmin,[ce] Nishat Tasnim,[b] Asif Rahman Dipto,[b] Harinarayan Das,[f] Md. Nurul Amin,[g] N. M.-Mofiz Uddin Khan,[h] Ahsan Habib[b] and Mahmudur Rahman *[a]

Climate change-induced heat stress severely impedes potato (*Solanum tuberosum*) germination, threatening global food security. Here, we report the application of green-synthesized silver nanoparticles (AgNPs), fabricated using *Azadirachta indica* (neem) leaf extract, as nanopriming agents to enhance germination and thermotolerance. The green-synthesized AgNPs exhibited a smaller crystallite size (9.7 nm) compared to chemically synthesized AgNPs (20.6 nm), with higher colloidal stability (zeta potential −55.2 mV *vs.* −35.7 mV). At the optimal priming concentration (5 mg L^{-1}), green AgNPs increased germination on the 12th day by 19% relative to chemical AgNPs and by 50% over hydroprimed controls. Under elevated temperature (32.2 °C), green AgNP-primed seeds maintained a consistent 10% higher germination rate than controls and showed faster radicle emergence. ICP-MS confirmed greater nanoparticle uptake in primed seeds (144 ppm Ag for green AgNPs *vs.* 105 ppm for chemical AgNPs, compared to 1.98 ppm in hydroprimed seeds). Enhanced water uptake was also evident, with an 82% increase in seed mass after green AgNP priming compared to 44% in hydroprimed seeds. A preliminary techno-economic analysis confirmed the superior cost-effectiveness of the green synthesis route. Collectively, these findings establish green-synthesized AgNP nanopriming as a cost-effective, sustainable, and biologically superior strategy to improve potato germination and heat stress resilience, offering a promising avenue for climate-smart agriculture.

Received 27th June 2025
Accepted 1st October 2025

DOI: 10.1039/d5ra04571a

rsc.li/rsc-advances

Open Access Article. Published on 21 October 2025. Downloaded on 4/29/2026 4:40:25 PM.
This article is licensed under a Creative Commons Attribution-NonCommercial 3.0 Unported Licence.

Introduction

As the global population continues to rise, ensuring sufficient food production to meet demand has become a critical challenge. By 2050, food production is expected to increase by approximately 50% compared to 2012 levels to meet the demands of the rapidly expanding population.[1] However, climate change, particularly the rise in global temperatures, poses a significant obstacle to achieving this goal.[2] Global temperatures have risen by 1.1 °C since preindustrial times, with faster warming over land areas.[3] This trend threatens potato (*Solanum tuberosum*) production, as heat stress reduces tuber yield and quality. Without adaptation, global yields may drop by 18–32%.[4] Potato germination and early seedling establishment are among the most vulnerable stages to rising temperatures, as tuber sprouting is strongly dependent on cool soil conditions, typically between 15–20 °C.[5] Under higher temperatures, dormancy release is delayed, sprouting becomes irregular, and physiological defects such as small or weak sprouts are more common.[6] Experimental evidence indicates that heat stress during germination can reduce subsequent tuber initiation and final yield potential by 20–30%, even if later growth conditions are favorable.[5,7] In areas, where potato is sown during the short winter season, increasing minimum temperatures rising by about 0.18 °C per decade in winter are already narrowing the suitable window for uniform germination.[3] Ranked as the third most significant food crop worldwide, following rice and wheat, potatoes are integral to ensuring global food security. Failure at the germination stage poses serious risks to both food security and rural livelihoods.[8] Thus,

[a]*Department of Electrical and Electronic Engineering, Dhaka University of Engineering & Technology, Gazipur-1707, Bangladesh. E-mail: m.rahman@duet.ac.bd*
[b]*Department of Electrical and Electronic Engineering, University of Dhaka, Dhaka-1000, Bangladesh*
[c]*Semiconductor Technology Research Centre, University of Dhaka, Dhaka-1000, Bangladesh*
[d]*Department of Computer Science and Engineering, Daffodil International University, Dhaka-1216, Bangladesh*
[e]*Department of Robotics and Mechatronics Engineering, University of Dhaka, Dhaka-1000, Bangladesh*
[f]*Bangladesh Atomic Energy Commission, Dhaka-1000, Bangladesh*
[g]*Department of Applied Chemistry and Chemical Engineering, University of Dhaka, Dhaka-1000, Bangladesh*
[h]*Department of Chemistry, Dhaka University of Engineering & Technology, Gazipur-1707, Bangladesh*
† The authors contributed equally to this work.

© 2025 The Author(s). Published by the Royal Society of Chemistry

Open Access Article. Published on 21 October 2025. Downloaded on 4/29/2026 4:40:25 PM. This article is licensed under a Creative Commons Attribution-NonCommercial 3.0 Unported Licence.

the development of heat-resistant potato seed varieties capable of maintaining strong sprouting and seedling vigor under elevated temperatures is an essential adaptation strategy to sustain potato production under ongoing climate change.

Nanomaterials have recently emerged as a promising approach to addressing these challenges in agriculture. Due to their unique ability to penetrate plant tissues, nanomaterials can enhance crop growth by improving nutrient absorption, optimizing water uptake, and suppressing disease outbreaks.[9] Nanopriming, an emerging application of nanotechnology, has demonstrated considerable potential to enhance crop resilience and boost productivity.[10] Nanopriming is a seed soaking technique involving the immersion of seeds in nanoparticle solutions for a specified duration, which enhances the germination rate and plant growth of the treated seeds.[11] Studies indicate that green-synthesized nanoparticles exhibit superior efficacy in nanopriming compared to chemically synthesized nanoparticles.[12] Kummara *et al.* demonstrated higher biocompatibility for green silver nanoparticles (AgNPs) compared to chemically synthesized AgNPs, which helps to improve germination rate and growth of the nanoprimed seeds.[13] The presence of capping agents in green-synthesized nanoparticles results in decreased agglomeration, ultimately leading to a reduction in particle size.[14] Moreover, a surface coating on Ag nanoparticles can effectively inhibit further oxidation by providing a protective barrier against environmental exposure.[15] Smaller nanoparticles can effectively penetrate the outer layer of seeds, resulting in superior performance of green-synthesized nanoparticles in nanopriming.[16]

Nanomaterials contribute to enhancing plant resistance against both biotic and abiotic stresses, thereby supporting the sustainability of agricultural ecosystems and minimizing crop losses associated with adverse environmental stressors.[17] Drought represents a critical ecological challenge that compromises crop productivity and nutrient composition. Research indicates that AgNPs contribute to enhancing plant resilience against both drought and saline stress conditions.[18] According to Ahmed *et al.*, AgNP-treated wheat plants exhibited enhanced chlorophyll stability index, leaf succulence, leaf K content, stomatal conductance, and increased water retention under drought stress.[19] Nejatzadeh *et al.* reported that the use of AgNP on *Satureja hortensis* significantly increased germination rate in the presence of salinity stress.[20] Additionally, the green synthesis approach for AgNP offers significant environmental benefits over conventional chemical methods.[21] By utilizing plant-derived reducing agents, this method avoids toxic reagents and harsh reaction conditions, resulting in a more sustainable and eco-friendly process.[22] Unlike chemically synthesized AgNPs, which often require energy-intensive procedures and generate hazardous byproducts, plant-mediated synthesis operates under ambient conditions, minimizes waste, and yields nanoparticles with biodegradable capping layers.[23] These attributes not only reduce environmental contamination risks but also align with the principles of green chemistry, making biofabricated AgNPs a more sustainable choice for agricultural applications. Despite the well-established significance of green-synthesized AgNPs on many aspects of abiotic stress tolerance, to the best of our knowledge, their potential in conferring resilience to extreme heat conditions remains largely unexplored, highlighting the need for further investigation in this domain.

Azadirachta indica (neem) has emerged as a potent source of diverse bioactive compounds, making it particularly effective for the green synthesis of silver nanoparticles (AgNPs).[24] Among its phytochemicals, terpenoids and flavonoids play a pivotal role not only reducing silver ions but also stabilizing and capping the resulting nanoparticles.[25] To enable a comparative evaluation, we initially explored AgNP synthesis using a range of plant extracts, including *Solanum lycopersicum* (tomato) leaves, peels of *Solanum tuberosum* (potato) and tried to follow protocols established in recent literature.[26,27] Although these methods have shown promise, our experiments yielded suboptimal results likely due to procedural deviations, environmental variables, or other experimental limitations. In contrast, neem consistently produced nanoparticles with desirable physicochemical traits, including smaller size, spherical morphology, and stable zeta potential. Other extracts either failed to form stable nanoparticles or led to significant agglomeration. The reduced efficacy observed with certain extracts may stem from minor inconsistencies in extraction protocols or natural variations in phytochemical content factors often influenced by geography, seasonality, or environmental conditions. Such variability can significantly impact nanoparticle synthesis and stability, as noted in prior studies.[28,29] Thus, while *Azadirachta indica* was initially selected for its known phytochemical richness and antioxidant profile, our findings further underscore its superior performance in green nanoparticle synthesis within our experimental framework.[30]

In this work, AgNPs were synthesized using an environment-friendly green synthesis method using *Azadirachta indica* (neem) leaf extract, and the effectiveness of these AgNPs as a nanopriming agent was then evaluated on *Solanum tuberosum* (potato) seeds. The performance of green-synthesized AgNPs was compared with chemically synthesized AgNPs to evaluate their relative effectiveness. Fig. 1 illustrates a schematic representation of the synthesis and comparative efficacy of green and chemically synthesized AgNPs in enhancing seed germination. The top panel (a) depicts the green synthesis procedure where bioactive flavonoids from neem leaf extract act as natural reducing and capping agents, yielding stable and biocompatible AgNPs with uniform morphology.[30] In contrast, the middle panel (b) shows the conventional chemical synthesis process using sodium citrate, which produces AgNPs with less tailored surface properties. The bottom panel (c) highlights the functional benefits of green-synthesized AgNPs in agricultural applications, demonstrating how nanoprimed seeds exhibit enhanced germination vigor and robust seedling development compared to traditional hydropriming methods. This schematic highlights the potential of plant-mediated synthesis to produce agriculturally superior nanomaterials, leveraging nature's reducing agents for sustainable crop resilience.

From the experimental results, we found an increase of 19% in germination rate for green AgNPs compared to chemically synthesized AgNPs. Both green and chemically synthesized NPs

© 2025 The Author(s). Published by the Royal Society of Chemistry

Open Access Article. Published on 21 October 2025. Downloaded on 4/29/2026 4:40:25 PM.
This article is licensed under a Creative Commons Attribution-NonCommercial 3.0 Unported Licence.

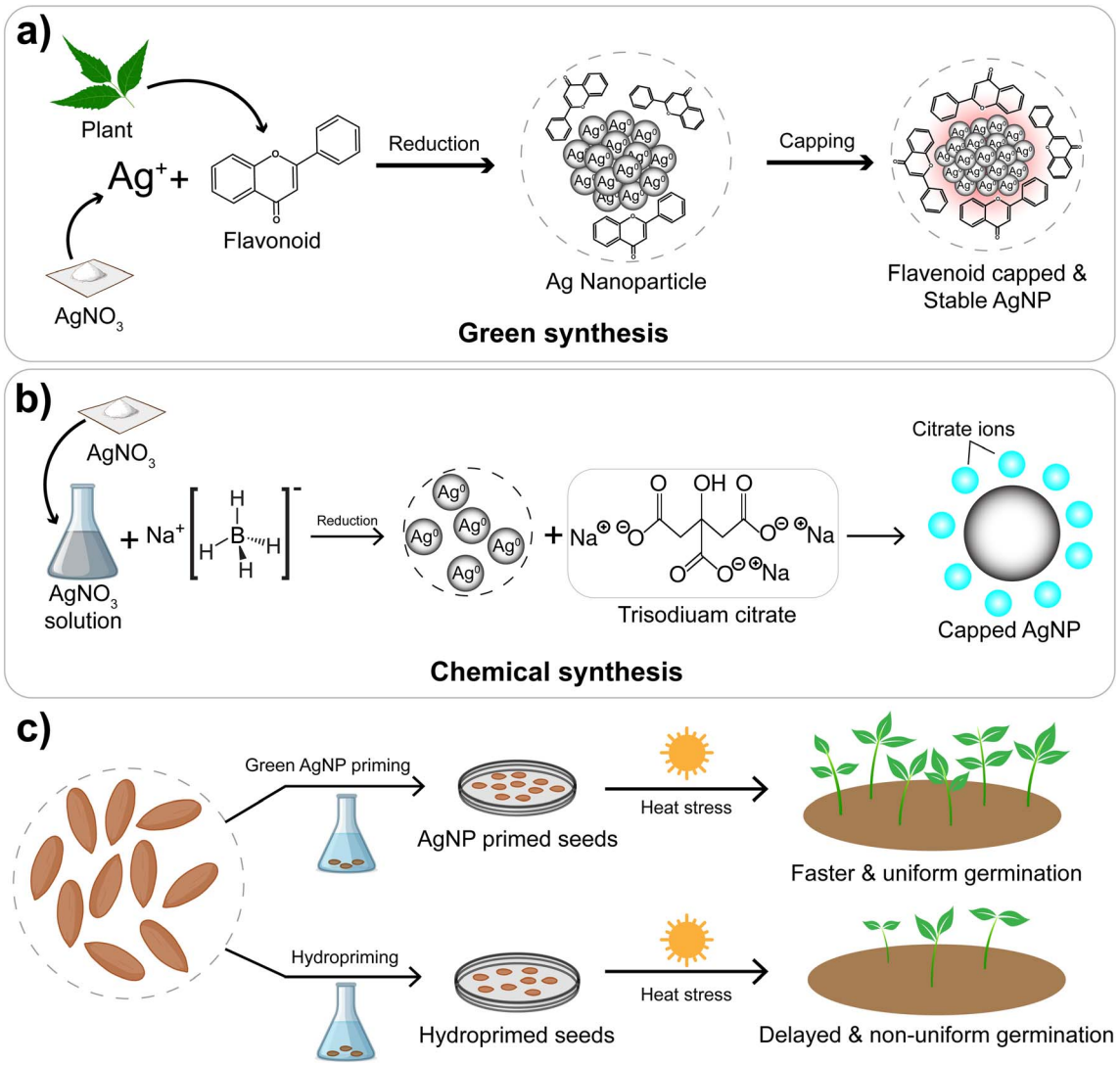

Fig. 1 Impact of nanopriming on seed germination and seedling growth. (a) Formation of AgNPs *via* green synthesis. (b) Formation of AgNPs *via* chemical synthesis. (c) Enhanced heat stress tolerance observed in seeds treated with green-synthesized AgNPs.

were characterized using X-ray diffraction, UV-visible spectroscopy, Fourier transform infrared (FTIR) spectroscopy, field emission scanning electron microscopy (FESEM), and dynamic light scattering (DLS). The characterization results indicate that the green-synthesized method produces smaller-sized AgNPs, which could potentially be the primary factor contributing to their superior nanopriming outcomes compared to chemically synthesized AgNPs. To investigate the effectiveness of AgNPs on heat stress resilience, the germination rate of potato seeds was monitored under different ambient temperatures. Control experiments at different dosages of AgNPs comparing hydroprimed, chemically synthesized AgNP-treated, and green-synthesized AgNP-treated seeds revealed optimal germination enhancement at 5 mg L^{-1}, which demonstrated maximum viability across all treatments. Based on this performance benchmark, the 5 mg L^{-1} concentration was selected for subsequent heat stress experiments. Under elevated temperature conditions, green-synthesized AgNPs exhibited superior heat tolerance effects, maintaining a 10% higher germination rate compared to the hydroprimed case with more vigorous seedling growth. These findings offer valuable insight into the promising role of Ag nanoparticles in sustainable agriculture mitigating the harmful effect of climate change.

Materials and methods

Synthesis of silver nanoparticles

Materials. The precursor materials used in this study included silver nitrate ($AgNO_3$, 99.5%), powdered trisodium citrate ($Na_3C_6H_5O_7$), and sodium borohydride ($NaBH_4$). All these chemicals were sourced from Labtex Bangladesh. Deionized water (DI) and ethanol (C_2H_5OH) were used as solvents. All reagents and chemicals were of analytical grade and were used without further purification.

Preparation of leaf extract. Fresh neem (*Azadirachta indica*) leaves were collected from the Dhaka University campus and thoroughly washed with sterile water to remove impurities. Next, the cleaned leaves were blended with deionized water to

Open Access Article. Published on 21 October 2025. Downloaded on 4/29/2026 4:40:25 PM. This article is licensed under a Creative Commons Attribution-NonCommercial 3.0 Unported Licence.

form a smooth paste. Subsequently, the paste was heated at 70 °C for 30 minutes to extract the active compounds. Once cooled to room temperature, the mixture was filtered using Whatman filter paper. Finally, the resulting filtrate was stored in a refrigerator for subsequent experiments.

Preparation of silver nanoparticles (AgNPs). To synthesize green silver nanoparticles (AgNPs), 5 mL of neem leaf extract was added to 100 mL of 1 mM silver nitrate ($AgNO_3$) solution. The mixture was stirred continuously with a magnetic stirrer for one hour to facilitate thorough reduction. The pH of the green synthesis environment was 5.9, indicating a slightly acidic solution. After stirring, the solution was wrapped in aluminum foil and stored in a dark place to minimize light exposure. The mixture was then refrigerated for 24 hours to allow the nanoparticles to stabilize and mature. A color change was observed after 24 hours, changing from yellowish-brown to thick brown, indicating the formation of AgNPs from silver ions. The synthesized nanoparticles were then analyzed using UV-vis spectroscopy.

For the chemical synthesis of AgNPs, trisodium citrate (TSC) was used as a stabilizer. A 50 mL solution of 1 mM $AgNO_3$ was prepared and stirred for 5 minutes to ensure complete dissolution. Subsequently, 50 mL of 1 mM TSC was added to the solution. Following this, 3 mL of 4 mM $NaBH_4$ was added dropwise to carefully control the reaction rate. Here, $NaBH_4$ acted as a reducing agent. The pH of the chemical synthesis environment was 8.1, suggesting a mildly alkaline solution. A color change from colorless to deep brown was observed, confirming the formation of AgNPs. The synthesized AgNPs were then transferred to a storage container and analyzed using UV-vis spectroscopy.

Characterization techniques. The synthesized samples were characterized using a range of analytical techniques. Gas Chromatography-Mass Spectrometry (GC-MS) analysis was performed using the electron impact ionization (EI) method on a GC-17A Gas Chromatograph (Shimadzu, Japan) coupled with a GCMS-QP 5050A Mass Spectrometer. A fused silica capillary column, with a temperature range from 40 °C to 250 °C and a port temperature of 250 °C at a constant pressure of 100 kPa, was utilized with a flow rate of 20 milliliters per minute. The full scan acquisition range was from 40 to 450 atomic mass units, and the compounds were identified by matching spectra with the National Institute of Standards and Technology (NIST) 127 and NIST 147 library data. UV-visible absorbance spectra were collected using a UV-2600i UV-Vis-NIR spectrometer (SHIMADZU), covering wavelengths between 200 and 800 nanometers. The surface chemistry of the samples was investigated by X-ray Photoelectron Spectroscopy (XPS) using a Thermo Fisher Scientific XPS spectrometer, operating at a pressure of 7×10^{-7} millibar and employing monochromatic aluminum Kα radiation (1486.68 eV). The samples, in powdered form, were mixed with ethanol and drop-cast onto a glass slide for analysis. Fourier Transform Infrared (FTIR) spectra were recorded using an IR Prestige-21 spectrometer (SHIMADZU) within the wavenumber range of 4000 to 400 centimeters inverse to confirm the presence of functional groups in the nanoparticles. X-ray Diffraction (XRD) analysis was conducted using a high-temperature X-ray diffractometer (model: PW 3040-X'Pert PRO, Philips), with copper Kα radiation ($\lambda = 0.15418$ nanometers) in the 10–80° range. Field Emission Scanning Electron Microscopy (FESEM) was employed for morphological analysis, and Energy Dispersive X-ray (EDX) was performed using the same equipment (high-resolution FESEM from the ZEISS Sigma family) to determine the elemental composition of the nanoparticles. For Transmission Electron Microscopy (TEM) analysis, a dilute nanoparticle dispersion was drop-cast onto an electron-transparent carbon-coated copper grid and dried before imaging. Dynamic Light Scattering (DLS) was used to measure the hydrodynamic size and zeta potential of the samples, providing insight into their colloidal stability. Lastly, Inductively Coupled Plasma-Mass Spectrometry (ICP-MS) (PerkinElmer, Model: NexION 2000, USA) was used for the quantification of trace metals, with the sample entering the argon plasma at a flow rate of 0.85 milliliters per minute. The quadrupole mass detector analyzed the trace metal ions by their mass-to-charge ratio (m/z). An ICP multi-element standard solution XIII (Merck, Germany) was used to create a calibration curve at parts per billion levels, and internal standards were introduced to mitigate potential errors such as instrumental drift, matrix effects, and variations in sample introduction.

Seed selection. We focused on BARI TPS-1 caste of *Solanum tuberosum* for our experiment. TPS, sourced from the Tuber Crops Research Centre in Gazipur, offers advantages for breeding new varieties and eliminating the need for storing seed potatoes.

Preparation of priming solution and seed priming method. The phytosynthesized AgNPs, chemically synthesized AgNPs, and $AgNO_3$ were utilized for seed priming at varying concentrations (0.5, 1, 5, and 10 mg L^{-1}). Fresh priming solutions were prepared by dispersing the respective nanoparticles in deionized water using ultrasonic vibration (100 W, 40 kHz) for 30 minutes. Healthy, uniform-sized *Solanum tuberosum* (TPS) seeds were selected and thoroughly washed under running tap water to ensure cleanliness. Afterward, the seeds were gently dried with tissue paper to remove excess moisture that might interfere with the priming process. The cleaned seeds were then soaked in the $AgNO_3$ or AgNPs priming solutions for 8 hours, while seeds soaked in distilled water, defined as hydropriming, were designated as control.

Germination assay

Germination tests were carried out on primed and hydroprimed seeds in triplicate. Briefly, sterile filter paper (Whatman No. 1) was placed in sterile plastic Petri dishes (90 × 15 mm) and moistened with 5 mL of deionized water. Thirty seeds were evenly placed in each dish, then covered with lids and sealed with Parafilm to prevent moisture loss. The dishes were incubated in the dark at 29 ± 2 °C to promote germination. Germination was evaluated by observing the appearance of the radicle, with observations recorded every 24 hours over a 10-day period. To maintain moisture, 5 mL of distilled water was added to each dish every other day.

© 2025 The Author(s). Published by the Royal Society of Chemistry

Open Access Article. Published on 21 October 2025. Downloaded on 4/29/2026 4:40:25 PM.
This article is licensed under a Creative Commons Attribution-NonCommercial 3.0 Unported Licence.

Heat stress was induced by placing the samples in an incubator with precise control of temperature. The incubator was built with a light bulb, a temperature sensor and an Arduino Uno. The incubator maintained stable elevated temperatures, ensuring uniform environmental conditions throughout the experiment. This precise regulation of temperature minimized variability and allowed for accurate assessment of the effects of heat stress on the samples.

Statistical analysis

All experiments were conducted in triplicate. One-way analysis of variance (ANOVA) was performed using IBM SPSS version 27. Data are presented as mean ± standard error of mean (SEM) ($\text{SEM} = \frac{\text{SD}}{\sqrt{n}}$, where SD is the sample standard deviation and n is the sample size). Significant differences were tested and means were compared using two-tailed independent samples Student's *t*-test. Data visualization and graph generation were carried out using Origin 2021 software.

Results and discussion

Phytochemical screening of the leaf extract

The phytochemicals identified in the gas chromatography-mass spectroscopy (GC-MS) analysis of the leaf extract of *Azadirachta indica*, as displayed in Fig. 2, play pivotal roles in the synthesis of AgNPs by acting as reducing, stabilizing, and capping agents. Compounds such as papaveroline, 2′-bromo-, tetramethyl(ether); pentadecanoic acid, 13-methyl-, methyl ester; L-proline, *n*-heptafluorobutyryl-, dodecyl ester; benzoic acid, *p*-((1-(dimethylcarbamoyl)ethyl)amino)-, ethyl ester; and 4-methylesculetin are likely involved in both reducing Ag^+ to Ag^0 and capping the AgNPs. These carboxylic acid derivatives and esters provide hydrogen atoms or electrons, reducing Ag^+ ions into elemental Ag^0 nanoparticles.[31] Additionally, the long-chain hydrocarbons, ethers, or carbonyl functional groups of these compounds bind to the nanoparticle surface, preventing aggregation and stabilizing their structure.[32] Flavonoids, such as *N*-methylcoclaurine and 3,4-methylenedioxycinnamic acid, also act as capping agents to prevent agglomeration of the AgNPs.[33]

Synthesis and characterization of AgNPs using leaf extract

The efficacy of nanoparticles as seed priming agents in enhancing seed germination and plant development is governed by various factors, including particle size, morphology, surface functionality, and stability. These properties, which significantly influence the interaction between nanoparticles and seeds, are determined by the synthesis method. In this study, silver nanoparticles are synthesized using both green and chemical methods, with variations in the reducing agents to modulate nanoparticle characteristics. The synthesized

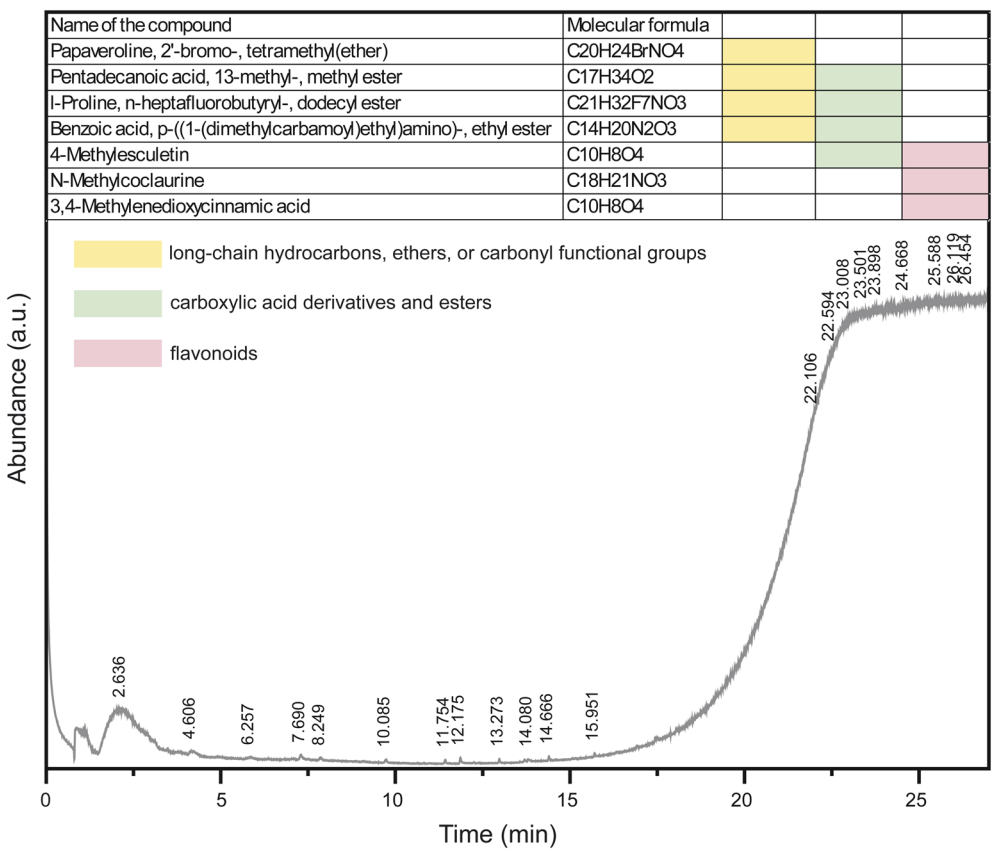

Fig. 2 Phytoconstituents detected in the leaf extract of *Azadirachta indica* using gas chromatography-mass spectrometry.

Open Access Article. Published on 21 October 2025. Downloaded on 4/29/2026 4:40:25 PM. This article is licensed under a Creative Commons Attribution-NonCommercial 3.0 Unported Licence.

nanoparticles are then thoroughly characterized to ensure reproducibility of the nanopriming process and to gain insights into their physical and chemical properties.

In the present investigation, *Azadirachta indica* (neem) leaf extract, rich in antioxidants, is selected for the green synthesis of silver nanoparticles. The reaction between the leaf extract and silver nitrate solution resulted in a characteristic color change from yellow to brown (see inset Fig. 3a(i)), a visual indicator of AgNP formation.[13] This color change is attributed to the excitation of surface plasmon vibrations within the synthesized AgNPs.[13,34] In contrast, chemically synthesized AgNPs, prepared using silver nitrate and sodium borohydride as a reducing agent, exhibited a colorless to dark brown appearance (inset Fig. 3a(ii)). UV-Vis spectroscopic analysis (Fig. 3a) confirms the successful synthesis of AgNPs in both cases, with distinct surface plasmon resonance (SPR) peaks observed at 417 nm and 396 nm for green and chemically synthesized AgNPs, respectively. Additionally, the absence of additional peaks in the spectra suggests the absence of impurities in either synthesis method.[16] However, the broad nature of the SPR peak in the green synthesized AgNPs indicates a polydisperse distribution of particle sizes, likely influenced by variations in the phytochemical composition and reaction conditions within the neem leaf extract.[34]

To confirm the elemental composition of the constituent atoms and detect any potential foreign impurities, energy-dispersive X-ray spectroscopy (EDX) was utilized. The strong signals corresponding to silver (Ag) in the EDX spectrum (see Fig. 3) confirm the successful synthesis of AgNPs through both green and chemical routes. The presence of carbon (C) and oxygen (O) peaks in the spectrum for green-synthesized AgNPs is attributed to the capping agents, which can be validated by the GC-MS results of the leaf extract. For chemically synthesized AgNPs, the carbon and oxygen peaks are similarly attributed to the citrate capping agent. Additionally, the presence of a sodium (Na) peak in the spectrum for chemically synthesized AgNPs indicates residual elements from the synthesis process. Notably, the oxygen peak is much more pronounced compared to the carbon peak in chemically synthesized AgNPs, suggesting the possible presence of oxidized silver.

To investigate the surface electronic structure, composition, and bonding configuration of the AgNP samples, X-ray photoelectron spectroscopy (XPS) was performed. The survey spectrum in Fig. 4a confirmed the presence of silver (Ag), oxygen (O), and carbon (C) in both the green and chemically synthesized AgNPs. While the oxygen and carbon signals are clearly evident, the silver signal is relatively weak in the XPS survey spectrum. This attenuation of the Ag 3d signal suggests that the surface of the AgNPs is coated with organic molecules derived from the plant extract.[35] The deconvoluted spectrum for the green-synthesized AgNPs in Fig. 4b shows two peaks at 374 eV and 368 eV, which correspond to Ag 3d3/2 and Ag 3d5/2, respectively. These peaks result from the spin-orbital splitting of the Ag 3d components, confirming the successful formation of metallic silver nanoparticles through the reduction of silver salt by the plant extract.[36] A similar pattern is observed for the chemically synthesized AgNPs, where citrate ions serve as the reducing agent. The deconvoluted peaks in both spectra for O 1s in Fig. 4c correspond to the C–OH moiety in aliphatic and aromatic species, appearing at 532.1 eV and 532.9 eV, respectively. In the C 1s region for the green-synthesized AgNPs, shown in Fig. 4d, the deconvolution reveals peaks corresponding to C=O, C–O, and C–C bonds. These peaks confirm the presence of organic materials, such as capping agents, on the nanoparticle surface. Similarly, for the chemically synthesized AgNPs, the same peaks are observed, indicating the presence of citrate ions as capping agents.

To identify the functional groups involved in the interaction between metal nanoparticles and phytochemicals, FTIR results of green and chemically synthesized AgNPs were analyzed.[37] The FTIR spectrum of green-synthesized AgNPs (Fig. 5a) reveals a strong peak in the range of 3430–3600 cm^{-1}, attributed to O–H stretching of hydrogen-bonded alcoholic and phenolic groups.[13,38] A weak peak around 1595 cm^{-1} corresponds to the C=C stretching bond of aromatic compounds.[39] Furthermore, a very weak band near 1450 cm^{-1} is likely associated with C=O stretching vibrations, which may originate from flavonoid compounds, potentially playing a crucial role in the effective capping and stabilization of the synthesized AgNPs.[13] In contrast, the FTIR spectrum of chemically synthesized AgNPs displays a sharp band at 1585 cm^{-1}, corresponding to the (C–C) and (C=C) stretching of aromatic groups. These findings indicate that the interactions of sodium citrate with Ag^{+} ions may not be optimal, and the structure of sodium citrate is

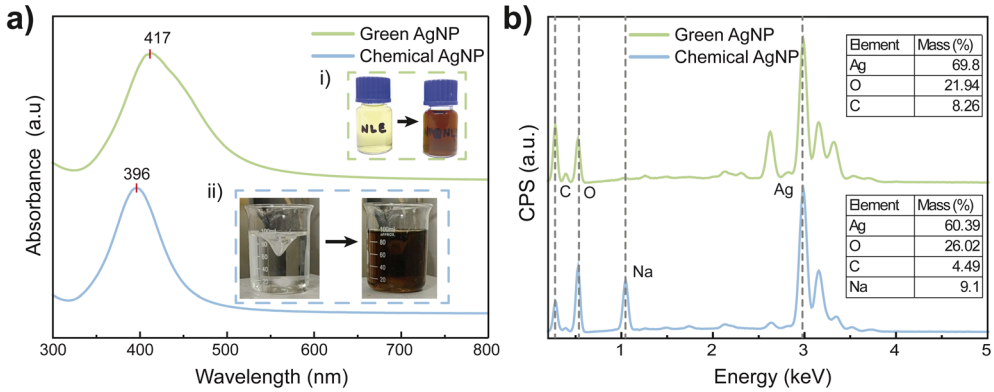

Fig. 3 (a) UV-visible spectra and (b) energy dispersive X-ray spectra of the green and chemically synthesized AgNPs.

© 2025 The Author(s). Published by the Royal Society of Chemistry

Open Access Article. Published on 21 October 2025. Downloaded on 4/29/2026 4:40:25 PM.
This article is licensed under a Creative Commons Attribution-NonCommercial 3.0 Unported Licence.

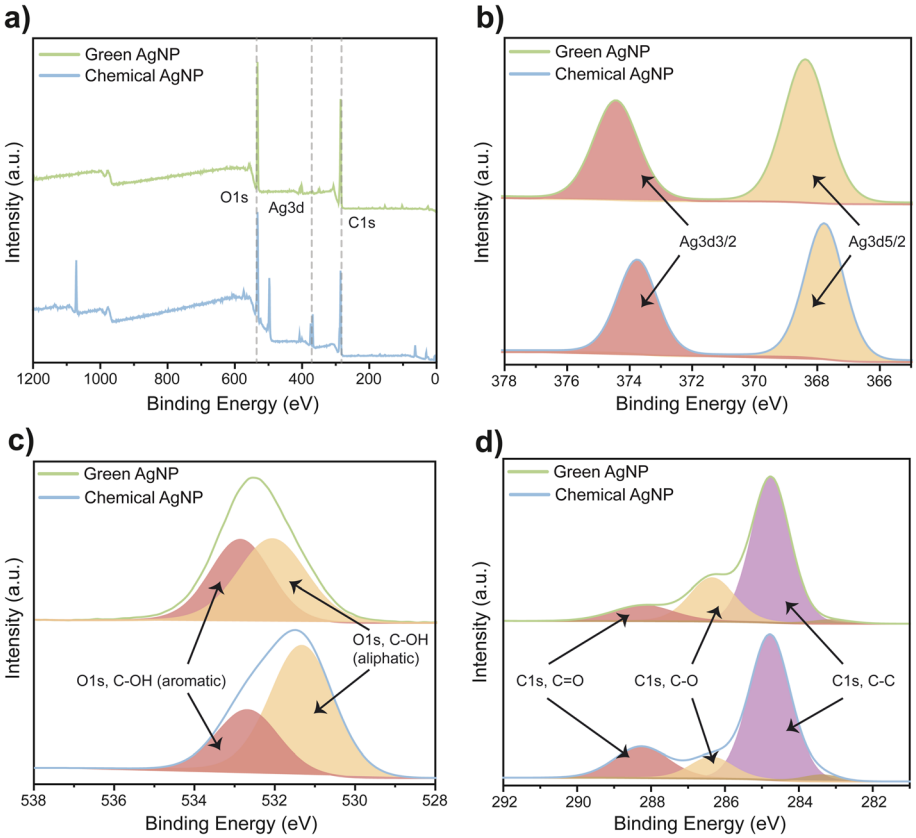

Fig. 4 XPS spectra of green and chemically synthesized AgNPs: (a) survey spectrum and high-resolution deconvoluted XPS spectra for (b) Ag, (c) O, and (d) C.

altered either during the reaction with Ag^{+} ions or after its binding to the AgNPs.[13]

To examine the phase identity, crystalline nature, and purity of the synthesized samples, we employ XRD analysis. The XRD patterns (see Fig. 5b) reveal three prominent diffraction peaks at 2θ values of 38.2°, 44.5°, and 64.6°, corresponding to the (111), (200), and (220) crystal planes, respectively, characteristic of the face-centered cubic crystal structure of metallic silver (JCPDS file no. 04-0783).[34,40] Additionally, minor unassigned peaks, indicated by asterisks, are also observed in the XRD pattern of the biosynthesized nanoparticles, potentially arising from the crystallization of a bioorganic phase on the nanoparticle surface.[13,34,40] The average crystallite size of the biosynthesized AgNPs, determined using the Debye–Scherrer equation based on the high-intensity (111) peak, is found to be approximately 9.65 nm. This value is significantly smaller than the average size of the chemically synthesized AgNPs, which is determined to be 20.55 nm. This reduced grain size of the green-synthesized AgNPs can be attributed to the broadening of the (111) diffraction peak observed in the XRD pattern.[41]

The size and morphology of AgNPs are significantly influenced by a range of factors, including pH, the concentration of

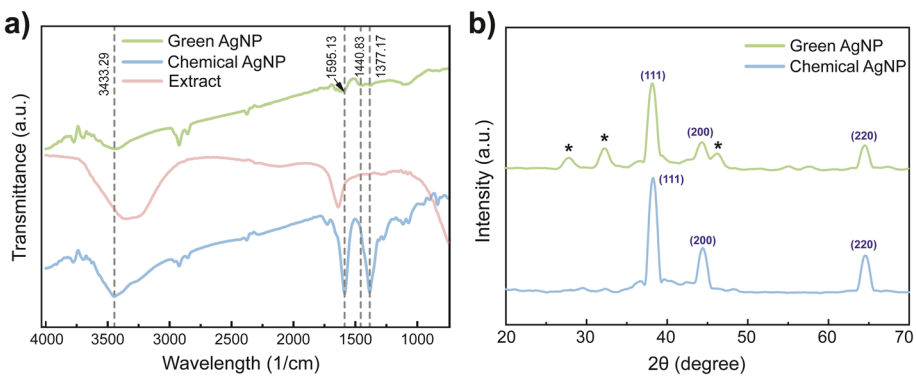

Fig. 5 (a) FTIR spectra and (b) X-ray diffraction patterns of the green and chemically synthesized AgNPs.

Open Access Article. Published on 21 October 2025. Downloaded on 4/29/2026 4:40:25 PM. This article is licensed under a Creative Commons Attribution-NonCommercial 3.0 Unported Licence.

reducing and $AgNO_3$ solutions, incubation time, temperature, and the chosen synthesis method.[13] In this study, FESEM is employed to investigate the size and morphological characteristics of AgNPs synthesized *via* both green and chemical methods. Fig. 6a clearly demonstrates that the green AgNPs exhibit a monodisperse, spherical morphology with an average diameter ranging from 20 to 25 nm, while the chemically synthesized AgNPs indicate a spherical shape and average diameter of 30–35 nm (Fig. 6c) along with very few bigger particles (90 nm). The crystallite size estimated from XRD analysis is notably smaller than the size determined from FESEM images for the corresponding AgNP samples. This discrepancy arises from the fundamental differences between the two techniques. XRD analysis, based on Debye–Scherrer's formula, provides an estimate of the size of individual crystallographic domains within the sample. In contrast, FESEM analysis measures the overall size of nanoparticles, including their surface morphology and distribution. The larger particle dimensions observed in FESEM images likely indicate that the nanoparticles are composed of multiple crystallographic domains rather than a single domain.[42]

To validate our claims, we analyzed the TEM results (see Fig. 6b), where the majority of the green-synthesized AgNPs are observed to be spherical in shape. In contrast, for chemically synthesized AgNPs, as shown in Fig. 6d, while most of the nanoparticles are spherical, a few exhibit an oval shape.

Complementing the SEM findings, we analyze the hydrodynamic size of synthesized AgNPs in aqueous solution using dynamic light scattering (DLS) to gain insights into their colloidal characteristics. It has been noticed that the hydrodynamic size distribution of AgNPs possesses a mean diameter of 55 nm for green and 75 nm for the chemical method (Fig. 7). These hydrodynamic diameters are larger than those observed by SEM, aligning with observations reported in earlier studies.[16,43]

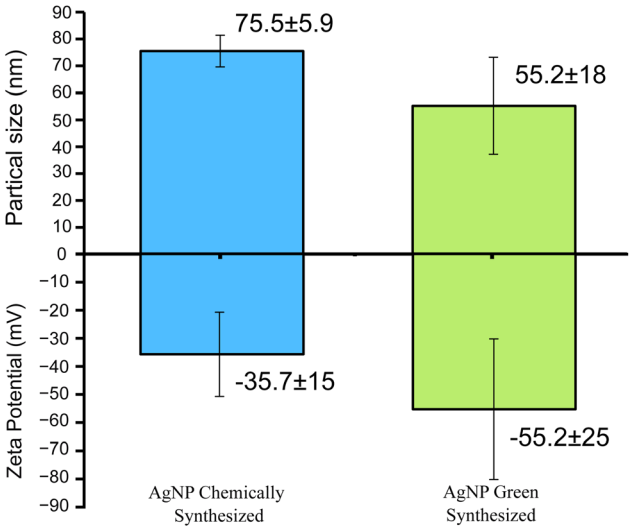

Fig. 7 Hydrodynamic size distribution and zeta potential measurement of green and chemically synthesized AgNPs by dynamic light scattering (DLS).

To assess the surface charge and colloidal stability of the synthesized AgNPs, zeta potential measurements were

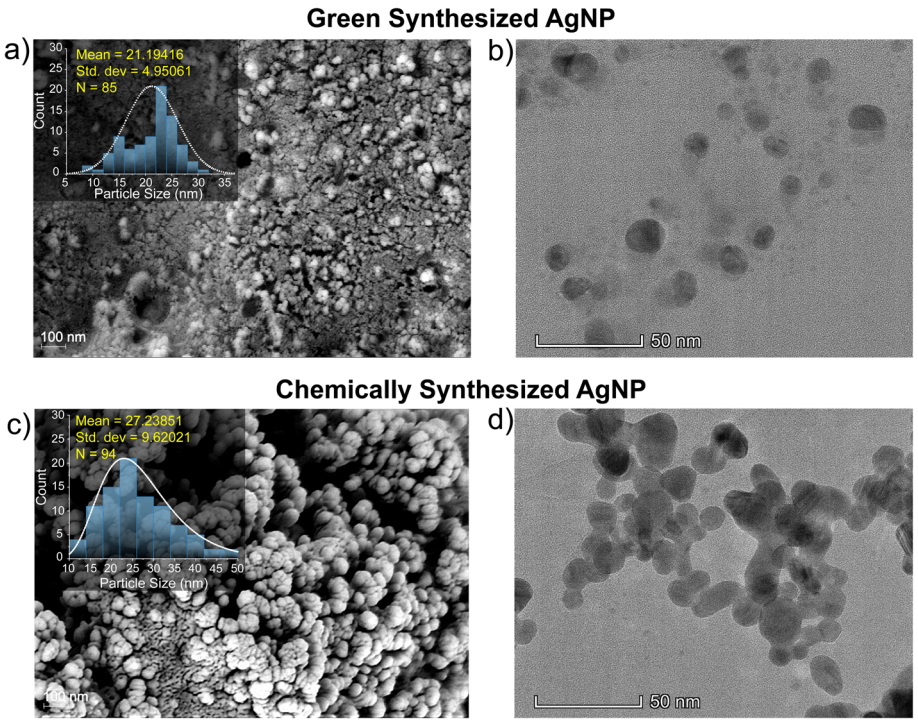

Fig. 6 FESEM images and particle size distribution of AgNPs. (a) FESEM image and particle size distribution for green synthesized AgNPs. (b) FESEM image and particle size distribution for chemically synthesized AgNPs. TEM images of (c) green synthesized AgNPs and (d) chemically synthesized AgNPs.

© 2025 The Author(s). Published by the Royal Society of Chemistry

Open Access Article. Published on 21 October 2025. Downloaded on 4/29/2026 4:40:25 PM. This article is licensed under a Creative Commons Attribution-NonCommercial 3.0 Unported Licence.

performed using DLS (see Fig. 7). The analysis reveals zeta potential values of −55.2 mV for green-synthesized AgNPs and −35.7 mV for chemically synthesized AgNPs. Previous studies suggest that nanoparticles with high zeta potential values (with an absolute value greater than 30 mV) generally exhibit high colloidal stability.[30,44] Accordingly, the observed negative zeta potential values, particularly the more pronounced value for green AgNPs, indicate superior stability of these nanoparticles. This enhanced stability aligns with the smaller hydrodynamic size observed for green-synthesized AgNPs, as particles with less negative zeta potential values are more susceptible to aggregation because of stronger interparticle interactions.[30]

Techno-economic analysis (TEA)

In the green synthesis method, the yield obtained after centrifuge and drying was approximately 7.1 mg per synthesis. In contrast, the chemical synthesis method produced a yield of approximately 3 mg per synthesis following the same processing steps. It should be noted that potential losses during centrifuge and recovery of the dried AgNPs may have affected the final yield measurements. According to Table 1, 1 mg of green synthesized AgNPs costs less compared to the chemically synthesized AgNP. So, we can conclude that green synthesis is more cost-effective. The cost of chemicals shown in Table 1 may fluctuate depending on market conditions. The chemical prices were obtained from the official websites of Sigma-Aldrich and Labtex Bangladesh.

The entire green synthesis process was carried out at ambient room temperature, without the need for heating, cooling, or energy-intensive equipment. This results in low energy input and supports environmentally sustainable processing. The quantity of nanoparticles synthesized from one batch can be used to treat a large number of seeds. This high output per batch enhances cost-effectiveness and minimizes the need for frequent synthesis.

Neem trees are widely available across both urban and rural areas in Bangladesh. Being a non-food, non-commercial species, neem collection does not compete with agriculture and is feasible at scale without environmental degradation.

While a full industrial-scale TEA is beyond the scope of this study, the preliminary data indicate that the process is cost-effective and eco-friendly under lab-scale conditions. These findings provide initial support for the sustainability claims made in this work.

Effect of AgNP on seed germination of potato

Previous studies have demonstrated that AgNPs can significantly influence seed germination and plant development in a dose-dependent manner, varying across plant species.[45,46] To investigate the differential effects of green (plant-mediated) and chemically synthesized AgNPs on potato seed germination, seeds were treated with various concentrations (0–10 mg L^{-1}) of AgNPs for 8 hours.

Our results (Fig. 8a) reveal that both types of AgNPs significantly enhance seed germination compared to the hydroprimed control at the 5 mg L^{-1} concentration. At this concentration, green AgNPs achieve a germination percentage of 57%, significantly higher than the 48% observed with chemically synthesized AgNPs and the 38% of the hydroprimed control. Based on these findings, 5 mg L^{-1} is determined to be the optimal AgNP concentration.

As shown in Fig. 8b, priming with 5 mg L^{-1} of green or chemically synthesized AgNPs accelerated early seed germination compared to $AgNO_3$-treated and hydroprimed seeds. By the 14th day, both nanoprimed groups reached high germination rates: 81% for green AgNPs and 77% for chemically synthesized AgNPs. This indicates that nanopriming significantly increased the overall germination percentage compared to both bulk-treated ($AgNO_3$) and hydroprimed seeds. Our findings corroborate previous research demonstrating that nanopriming accelerates seed germination.[16,47,48] This enhancement can be attributed to several factors, including increased water uptake due to the creation of nanopores on the seed surface. This increased water uptake stimulates the activity of dehydrogenase, a key enzyme in cellular respiration, leading to improved seed germination.[34,40] Additionally, Ag^+ ions can induce various biochemical changes in seeds, such as breaking dormancy, hydrolyzing or metabolizing inhibitors, and activating enzymes, thereby initiating the germination process.[49,50]

To verify the enhanced silver uptake, we compared the absorption of silver nanoparticles in nanoprimed potato seeds with hydroprimed controls using inductively coupled plasma-

Table 1 Raw material cost & extraction for AgNP synthesis

Material	Quantity	Price	Unit price	Quantity/synthesis	Price/synthesis
Green synthesized AgNP					
Neem leaves	—	$0	—	5 mL	$0
Silver nitrate	25 g	$250	$10 per g	0.017 g	$0.17
Total cost per synthesis					**$0.17**
Total cost per mg AgNP					**$0.0239**
Chemically synthesized AgNP					
Silver nitrate	25 g	$250	$10 per g	0.0085 g	$0.085
Sodium borohydride	100 g	$56.5	$0.565 per g	0.045 g	$0.0254
Trisodium citrate	500 g	$10.68	$0.0213 per g	0.072 g	$0.00153
Total cost per synthesis					**$0.11193**
Total cost per mg AgNP					**$0.03731**

Open Access Article. Published on 21 October 2025. Downloaded on 4/29/2026 4:40:25 PM.
This article is licensed under a Creative Commons Attribution-NonCommercial 3.0 Unported Licence.

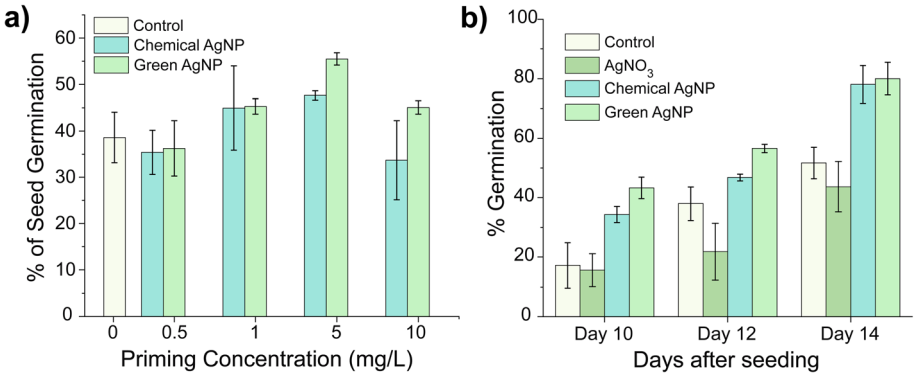

Fig. 8 Effect of green and chemically synthesized AgNPs on percentage of seed germination in potato seeds. (a) Seeds were treated with green and chemically synthesized AgNPs at different concentrations (0–10 mg L^{-1}) for 8 h, and germination was determined, and (b) effect of 5 mg L^{-1} treatments on potato seed germination. Data are mean ± SD from three independent experiments.

mass spectroscopy (ICP-MS). The silver concentration in chemically synthesized AgNP nanoprimed seeds was found to be 105 ppm, whereas hydroprimed seeds showed only 1.98 ppm. In the case of green-synthesized AgNPs, the silver concentration was 144 ppm, surpassing both the chemically synthesized AgNP nanoprimed seeds and the hydroprimed controls. These findings confirm that green-synthesized AgNP treatment significantly enhances silver uptake, providing a mechanistic basis for the observed improvements in seed germination and seedling development.

To illustrate the relative water uptake of nanoprimed and hydroprimed seeds, the weight of different seed samples (control and 5 mg L^{-1}) was measured before and after priming. For the hydroprimed seeds, a 44% increase in weight was observed after priming. In contrast, the nanoprimed seeds exhibited a weight increase of 82% for green-synthesized AgNPs and 60% for chemically synthesized AgNPs, highlighting the superior water uptake of the green-synthesized AgNP nanoprimed seeds.

It is also observed that green AgNPs exhibit a more pronounced stimulatory effect on germination, achieving the highest germination rate among all treatments. This enhanced effect may be attributed to the smaller size of green AgNPs compared to chemically synthesized AgNPs, as revealed by characterization results. Smaller particles may exhibit greater penetration through the seed coat, leading to improved interaction with cellular components.[16,30] At the optimal concentration, the pH of the nanopriming solutions was 7.18 for green-synthesized AgNPs and 7.39 for chemically synthesized AgNPs, indicating nearly neutral solutions that are unlikely to harm the soil. Based on these observations, 5 mg per L green AgNPs is selected for further investigation to assess how AgNP-primed seeds respond to heat stress during summer.

Effects of AgNPs on potato seed germination under heat stress

To investigate the effect of AgNP nanopriming on heat stress tolerance in potatoes, we examined seed germination and seedling emergence under varying temperatures. Compared to hydroprimed controls, AgNP-treated seeds exhibited superior performance across all tested temperatures as depicted in Fig. 9. At 29.97 °C and 67.8% relative humidity, we observed a near two-fold increase in germination rates by day 14 in the AgNP group, highlighting the nanoparticles' ability to maintain metabolic activity under thermal stress. This advantage became particularly evident at the higher stress threshold of 32.2 °C (61.39% humidity), where AgNP-primed seeds maintained a consistent 10% germination advantage over controls through the final observation period.

The germination timeline revealed important kinetics: seeds treated with AgNPs showed significantly faster root emergence, reaching 25–30% higher germination rates than untreated controls by day 10. This suggests that AgNP treatment may

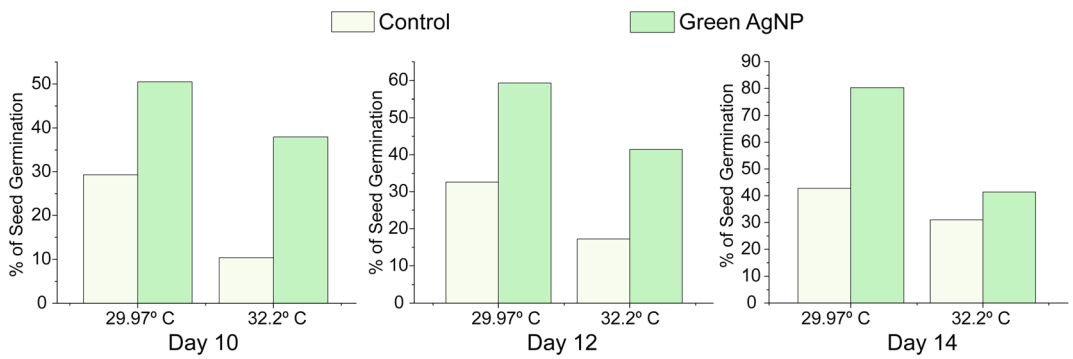

Fig. 9 Germination rate of potato seeds under varying environmental conditions.

© 2025 The Author(s). Published by the Royal Society of Chemistry

Open Access Article. Published on 21 October 2025. Downloaded on 4/29/2026 4:40:25 PM. This article is licensed under a Creative Commons Attribution-NonCommercial 3.0 Unported Licence.

improve water uptake or activate enzymes essential for germination. Moreover, while germination in control seeds slowed after day 12 at 32.2 °C, AgNP-treated seeds continued growing, indicating sustained protection against heat stress.

These results align with established mechanisms of nanoparticle-mediated stress protection, including ROS mitigation and membrane stabilization through antioxidant enzyme induction.[51,52] The superior performance of green-synthesized AgNPs likely stems from their smaller size and natural capping agents from neem extract, which may provide additional phytochemical benefits. Our findings suggest AgNP nanopriming could enhance potato cultivation in warming climates, though field validation remains essential to confirm these controlled-environment results.

Conclusion

This study highlights the promising application of nanopriming with AgNPs for potato seeds in agriculture. Our findings demonstrate that phyto-mediated AgNPs act as effective priming agents, significantly accelerating seed germination compared to conventionally synthesized AgNPs. Through systematic experimentation, we identified 5 mg L^{-1} as the optimal priming dose for both types of nanoparticles, with the smallest (green-synthesized AgNPs) yielding the most favorable results.

Furthermore, our results indicate that biologically synthesized AgNPs exerted a slight stress condition on the germination and growth of potatoes and winter vegetables under heat stress. Notably, the germination vigor of biosynthesized AgNP-treated seeds remained higher at the highest tested temperature (32.2 °C), whereas hydroprimed control seeds exhibited a lower germination rate in all cases.

The cost-effectiveness, biocompatibility, and tunability of AgNPs make them a viable option for future agricultural applications, particularly in nanopriming. However, further studies, including long-term nanotoxicology assessments, are necessary to validate these preliminary findings and develop standardized models for evaluating the long-term impact of AgNPs in seed priming. Establishing well-defined *in vivo* studies will be crucial for integrating AgNP-based priming techniques into sustainable agricultural practices.

Conflicts of interest

The authors declare no conflicts of interest.

Data availability

All data supporting the findings of this study are included within the manuscript. Additional datasets are available from the corresponding author upon reasonable request.

Acknowledgements

Mahmudur Rahman acknowledges research funding from the University Grants Commission of Bangladesh (Grant 2024–2025, CASR No. 79) through DUET, Gazipur. Ahsan Habib acknowledges support from the Ministry of Science and Technology, Bangladesh (Research Grant 2024–2025, SRG-242301). The authors thank the Semiconductor Technology Research Centre (STRC), University of Dhaka (DU) for synthesis facilities, the Department of Biomedical Engineering at Bangladesh University of Engineering and Technology for FESEM access, and the Centre for Advanced Research in Sciences (CARS), University of Dhaka (DU) for XRD and FTIR analysis.

References

1 Organization A, The state of food and agriculture 2016: Climate change, agriculture and food security, Food & Agriculture Organization of the UN (FAO), 2017.
2 G. Fischer, M. Shah, F. N. Tubiello and H. van Velhuizen, Socio-economic and climate change impacts on agriculture: An Integrated Assessment, 1990–2080, *Philos. Trans. R. Soc., B*, 2005, **360**, 2067–2083.
3 V. Masson-Delmotte, P. Zhai, A. Pirani, S. L. Connors, C. Péan, S. Berger, N. Caud, Y. Chen, L. Goldfarb, M. Gomis, *et al.*, *Climate Change 2021: the Physical Science Basis. Contribution of Working Group I to the Sixth Assessment Report of the Intergovernmental Panel on Climate Change*, 2021, vol. 2, p. 2391.
4 T. Handayani, S. A. Gilani and K. N. Watanabe, Climatic changes and potatoes: How can we cope with the abiotic stresses?, *Breed. Sci.*, 2019, **69**, 545–563.
5 R. J. Hijmans, The effect of climate change on global potato production, *Am. J. Potato Res.*, 2003, **80**, 271–279.
6 A. Dieme and M. O. Sy, Environmental, morphological and physiological factors analyzes for optimization of potato (Solanum tuberosum L.) microtuber in vitro germination, *Adv. Biosci. Biotechnol.*, 2013, **4**, 986–992.
7 D. Levy and R. E. Veilleux, Adaptation of potato to high temperatures and salinity-a review, *Am. J. Potato Res.*, 2007, **84**, 487–506.
8 O. Ortiz and V. Mares, *The Potato Genome*, Springer, 2017, pp. 1–10.
9 P. Wang, E. Lombi, F.-J. Zhao and P. M. Kopittke, Nanotechnology: a new opportunity in plant sciences, *Trends Plant Sci.*, 2016, **21**, 699–712.
10 W. Mahakham, A. K. Sarmah, S. Maensiri and P. Theerakulpisut, Nanopriming technology for enhancing germination and starch metabolism of aged rice seeds using phytosynthesized silver nanoparticles, *Sci. Rep.*, 2017, **7**(1), 8263.
11 A. Saini, R. Verma, R. Tiwari, A. Jain, A. Dandia, V. S. Gour, N. P. Lamba, S. C. Srivastava and M. S. Chauhan, Green synthesis of silver nanoparticle for catalytic applications and priming study by seed germination, *Sci. Rep.*, 2024, **14**, 20744.
12 S. H. Nile, M. Thiruvengadam, Y. Wang, R. Samynathan, M. A. Shariati, M. Rebezov, A. Nile, M. Sun, B. Venkidasamy, J. Xiao, *et al.*, Nano-priming as emerging seed priming technology for sustainable agriculture—

Open Access Article. Published on 21 October 2025. Downloaded on 4/29/2026 4:40:25 PM. This article is licensed under a Creative Commons Attribution-NonCommercial 3.0 Unported Licence.

recent developments and future perspectives, *J. Nanobiotechnol.*, 2022, **20**(1), 254.

13 S. Kummara, M. B. Patil and T. Uriah, Synthesis, characterization, biocompatible and anticancer activity of green and chemically synthesized silver nanoparticles–a comparative study, *Biomed. Pharmacother.*, 2016, **84**, 10–21.

14 K. Elumalai and S. Velmurugan, Green synthesis, characterization and antimicrobial activities of zinc oxide nanoparticles from the leaf extract of Azadirachta indica (L.), *Appl. Surf. Sci.*, 2015, **345**, 329–336.

15 M. S. Mostafa, M. M. H. Pranto, M. A. Islam and S. Islam, Design of a highly sensitive Ag–TiO_2-coated photonic crystal fiber-based refractive index sensor for anemia and diabetes detection, *J. Opt. Soc. Am. B*, 2025, **42**(10), 2306–2315.

16 S. Yeasmin, A. R. Dipto, A. B. Zakir, S. D. Shovan, M. A. H. Suvo, M. A. Bhuiyan, M. N. Amin, T. U. Rashid, S. Islam and A. Habib, Nanopriming and AI for Sustainable Agriculture: Boosting Seed Germination and Seedling Growth with Engineered Nanomaterials, and Smart Monitoring through Deep Learning, *ACS Appl. Nano Mater.*, 2024, **7**, 8703–8715.

17 M. Hassanisaadi, M. Barani, A. Rahdar, M. Heidary, A. Thysiadou and G. Z. Kyzas, Role of agrochemical-based nanomaterials in plants: Biotic and abiotic stress with germination improvement of seeds, *Plant Growth Regul.*, 2022, **97**, 375–418.

18 S. García-Sánchez, I. Bernales and S. Cristobal, Early response to nanoparticles in the Arabidopsis transcriptome compromises plant defence and root-hair development through salicylic acid signalling, *BMC Genomics*, 2015, **16**(1), 341.

19 F. Ahmed, B. Javed, A. Razzaq and Z.-U.-R. Mashwani, Applications of copper and silver nanoparticles on wheat plants to induce drought tolerance and increase yield, *IET Nanobiotechnol.*, 2021, **15**, 68–78.

20 F. Nejatzadeh, Effect of silver nanoparticles on salt tolerance of Satureja hortensis L. during in vitro and in vivo germination tests, *Heliyon*, 2021, **7**, e05981.

21 J. Palanisamy, V. S. Palanichamy, G. Vellaichamy, P. Perumal, J. Vinayagam, S. Gunalan, S. G. Prabhakaran, P. P. Thiraviam, F. Musthafa, A. K. Balaraman, *et al.*, A comprehensive review on the green synthesis of silver nanoparticles from marine sources, *Naunyn-Schmiedeberg's Arch. Pharmacol.*, 2025, 3409–3432.

22 M. Pirsaheb, T. Gholami, H. Seifi, E. A. Dawi, E. A. Said, A.-H. M. Hamoody, U. S. Altimari and M. Salavati-Niasari, Green synthesis of nanomaterials by using plant extracts as reducing and capping agents, *Environ. Sci. Pollut. Res.*, 2024, **31**, 24768–24787.

23 N. K. Sharma, J. Vishwakarma, S. Rai, T. S. Alomar, N. AlMasoud and A. Bhattarai, Green route synthesis and characterization techniques of silver nanoparticles and their biological adeptness, *ACS Omega*, 2022, **7**, 27004–27020.

24 S. Ahmed, M. Ahmad, B. L. Swami and S. Ikram, A review on plants extract mediated synthesis of silver nanoparticles for antimicrobial applications: a green expertise, *J. Adv. Res.*, 2016, **7**, 17–28.

25 P. Roy, B. Das, A. Mohanty and S. Mohapatra, Green synthesis of silver nanoparticles using Azadirachta indica leaf extract and its antimicrobial study, *Appl. Nanosci.*, 2017, **7**, 843–850.

26 T. R. Santiago, C. C. Bonatto, M. Rossato, C. A. Lopes, C. A. Lopes, E. S. G Mizubuti and L. P. Silva, Green synthesis of silver nanoparticles using tomato leaf extract and their entrapment in chitosan nanoparticles to control bacterial wilt, *J. Sci. Food Agric.*, 2019, **99**, 4248–4259.

27 Deepa, R. Dhanker, R. Kumar, S. S. Kamble, Kamakshi and S. Goyal, Biosynthesis and characterization of silver nanoparticles generated from peels of Solanum tuberosum (potato) and their antibacterial and wastewater treatment potential, *Front. Nanotechnol.*, 2023, **5**, 1213160.

28 J. Azmir, I. S. M. Zaidul, M. M. Rahman, K. M. Sharif, A. Mohamed, F. Sahena, M. H. A. Jahurul, K. Ghafoor, N. A. Norulaini and A. K. Omar, Techniques for extraction of bioactive compounds from plant materials: A review, *J. Food Eng.*, 2013, **117**, 426–436.

29 J. H. Goell and I. B. Hilton, CRISPR/Cas-based epigenome editing: advances, applications, and clinical utility, *Trends Biotechnol.*, 2021, **39**, 678–691.

30 M. S. Mostafa, S. Yeasmin, M. M. H. Pranto, S. M. Reza, T. U. Rashid, H. Das, M. Rahman and A. Habib, Annealing-induced optimization of green-synthesized ZnO nanoparticles for improved nanopriming in sustainable agriculture, *Nanoscale Adv.*, 2025, **7**, 5589–5600.

31 P. Uznanski, J. Zakrzewska, F. Favier, S. Kazmierski and E. Bryszewska, Synthesis and characterization of silver nanoparticles from (bis) alkylamine silver carboxylate precursors, *J. Nanopart. Res.*, 2017, **19**, 121.

32 A. K. Sidhu, N. Verma and P. Kaushal, Role of biogenic capping agents in the synthesis of metallic nanoparticles and evaluation of their therapeutic potential, *Front. Nanotechnol.*, 2022, **3**, 801620.

33 F. Quddus, A. Shah, J. Nisar, M. A. Zia and S. Munir, Neem plant extract-assisted synthesis of CeO 2 nanoparticles for photocatalytic degradation of piroxicam and naproxen, *RSC Adv.*, 2023, **13**, 28121–28130.

34 W. Mahakham, A. K. Sarmah, S. Maensiri and P. Theerakulpisut, Nanopriming technology for enhancing germination and starch metabolism of aged rice seeds using phytosynthesized silver nanoparticles, *Sci. Rep.*, 2017, **7**, 8263.

35 R. P. Illanes Tormena, M.-K. Medeiros Salviano Santos, A. Oliveira da Silva, F. M. Félix, J. A. Chaker, D. O. Freire, I. C. Rodrigues da Silva, S. E. Moya and M. H. Sousa, Enhancing the antimicrobial activity of silver nanoparticles against pathogenic bacteria by using Pelargonium sidoides DC extract in microwave assisted green synthesis, *RSC Adv.*, 2024, **14**, 22035–22043.

36 R. B. Patil and A. D. Chougale, Analytical methods for the identification and characterization of silver nanoparticles: A brief review, *Mater. Today: Proc.*, 2021, **47**, 5520–5532.

© 2025 The Author(s). Published by the Royal Society of Chemistry

Open Access Article. Published on 21 October 2025. Downloaded on 4/29/2026 4:40:25 PM. This article is licensed under a Creative Commons Attribution-NonCommercial 3.0 Unported Licence.

37 F. Faghihzadeh, N. M. Anaya, L. A. Schifman and V. Oyanedel-Craver, Fourier transform infrared spectroscopy to assess molecular-level changes in microorganisms exposed to nanoparticles, *Nanotechnol. Environ. Eng.*, 2016, **1**, 1–16.

38 J. A. Mazumder, E. Khan, M. Perwez, M. Gupta, S. Kumar, K. Raza and M. Sardar, Exposure of biosynthesized nanoscale ZnO to Brassica juncea crop plant: morphological, biochemical and molecular aspects, *Sci. Rep.*, 2020, **10**, 8531.

39 V. Ţucureanu, A. Matei and A. M. Avram, FTIR spectroscopy for carbon family study, *Crit. Rev. Anal. Chem.*, 2016, **46**, 502–520.

40 P. Acharya, G. K. Jayaprakasha, K. M. Crosby, J. L. Jifon and B. S. Patil, Nanoparticle-mediated seed priming improves germination, growth, yield, and quality of watermelons (Citrullus lanatus) at multi-locations in Texas, *Sci. Rep.*, 2020, **10**, 5037.

41 P. Kumari, A. Srivastava, R. K. Sharma, A. Saini, D. Sharma, J. S. Tawale and S. K. Srivastava, Facile synthesis and tailoring the structural and photoluminescence properties of ZnO nanoparticles via annealing in air atmosphere, *Mater. Today Commun.*, 2022, **32**, 103845.

42 R. N. Aljawfi, M. J. Alam, F. Rahman, S. Ahmad, A. Shahee and S. Kumar, Impact of annealing on the structural and optical properties of ZnO nanoparticles and tracing the formation of clusters via DFT calculation, *Arabian J. Chem.*, 2020, **13**, 2207–2218.

43 S. M. Savassa, N. M. Duran, E. S. Rodrigues, E. De Almeida, C. A. Van Gestel, T. F. Bompadre and H. W. P. de Carvalho, Effects of ZnO nanoparticles on Phaseolus vulgaris germination and seedling development determined by X-ray spectroscopy, *ACS Appl. Nano Mater.*, 2018, **1**, 6414–6426.

44 A. Brunelli, A. Foscari, G. Basei, G. Lusvardi, C. Bettiol, E. Semenzin, A. Marcomini and E. Badetti, Colloidal stability classification of TiO2 nanoparticles in artificial and in natural waters by cluster analysis and a global stability index: Influence of standard and natural colloidal particles, *Sci. Total Environ.*, 2022, **829**, 154658.

45 M. J. Firdhouse and P. Lalitha, Biosynthesis of silver nanoparticles and its applications, *J. Nanotechnol.*, 2015, **2015**, 829526.

46 K. S. Siddiqi, A. Husen and R. A. Rao, A review on biosynthesis of silver nanoparticles and their biocidal properties, *J. Nanobiotechnol.*, 2018, **16**, 14.

47 P. Rai-Kalal and A. Jajoo, Priming with zinc oxide nanoparticles improve germination and photosynthetic performance in wheat, *Plant Physiol. Biochem.*, 2021, **160**, 341–351.

48 K. V. Anand, A. Anugraga, M. Kannan, G. Singaravelu and K. Govindaraju, Bio-engineered magnesium oxide nanoparticles as nano-priming agent for enhancing seed germination and seedling vigour of green gram (Vigna radiata L.), *Mater. Lett.*, 2020, **271**, 127792.

49 M. Ghavam, Effect of silver nanoparticles on seed germination and seedling growth in Thymus vulgaris L. and Thymus daenensis Celak under salinity stress, *J. Rangel. Sci.*, 2018, **8**, 93–100.

50 Z. M. Almutairi and A. Alharbi, Effect of silver nanoparticles on seed germination of crop plants, *J. Adv. Agric.*, 2015, **4**, 283–288.

51 A. Manke, L. Wang and Y. Rojanasakul, Mechanisms of Nanoparticle-Induced Oxidative Stress and Toxicity, *Biomed Res. Int.*, 2013, **2013**, 1–15.

52 S. Sharma, V. K. Singh, A. Kumar and S. Mallubhotla, *Effect of Nanoparticles on Oxidative Damage and Antioxidant Defense System in Plants*, 2019.

© 2025 The Author(s). Published by the Royal Society of Chemistry